Optical Properties in Nonequilibrium Phase Transitions

T. Ao,[1] Y. Ping,[2] K. Widmann,[2] D. F. Price,[2] E. Lee,[1] H. Tam,[1] P. T. Springer,[2] and A. Ng[1,2]

[1]*Department of Physics & Astronomy, University of British Columbia, Vancouver, British Columbia, Canada*

[2]*Physics & Advanced Technologies, Lawrence Livermore National Laboratory, Livermore, California 94550, USA*

(Received 25 August 2004; revised manuscript received 4 April 2005; published 8 February 2006)

An open question about the dynamical behavior of materials is how phase transition occurs in highly nonequilibrium systems. One important class of study is the excitation of a solid by an ultrafast, intense laser. The preferential heating of electrons by the laser field gives rise to initial states dominated by hot electrons in a cold lattice. Using a femtosecond laser pump-probe approach, we have followed the temporal evolution of the optical properties of such a system. The results show interesting correlation to nonthermal melting and lattice disordering processes. They also reveal a liquid-plasma transition when the lattice energy density reaches a critical value.

DOI: 10.1103/PhysRevLett.96.055001 PACS numbers: 52.50.Jm, 52.25.Fi, 52.25.Os, 52.38.−r

Phase transitions are fundamental processes of nature. The most familiar among them are structural changes such as melting or freezing, vaporization or condensation, and sublimation that define the three states of matter, namely, solid, liquid, and gas. Understanding phase boundaries and transition kinetics has long been a focus of research in material science, chemistry, and biology. While most studies are concerned with the behavior of states in thermodynamic equilibrium, there is a growing interest in the investigation of nonequilibrium behavior over time scales pertinent to atomic and molecular motion, that is, femtosecond to picosecond. It holds the promise of discovering new phases and metastable states, chemical reaction pathways as well as biological functioning processes. It is also key to the understanding of radiation-induced damage thresholds that impact a broad range of technologies ranging from optics and electronics to biological imaging and microscopy. Experimental studies in such time scales have been both enabled and driven by advances in femtosecond lasers. They offer unparalleled temporal resolution for delineating the evolution of dynamical processes.

Ultrafast laser heating has been widely used to investigate phase changes in solid under nonequilibrium conditions, including nonthermal melting [1–6], lattice disordering [7], as well as desorption and ablation [8]. These studies were conducted at modest incident fluences (≤ 70 mJ/cm^2). Most [1–6,8] were made on thin films deposited on top of substrates where the spatially varying energy density resulting from nonuniform heating could not be quantified directly. Recently, isochoric and uniform heating of a solid by an intense femtosecond laser has been demonstrated using a freestanding, 25–30 nm thick gold foil in vacuum [9]. This renders it possible to characterize the heated state by its initial mass density ρ_0 and the excitation energy density $\Delta\varepsilon$ due to laser deposition. Both of these quantities are obtained from direct measurements without relying on model interpretations. Furthermore, vacuum insulation allows the heated state to be free from the effects of electron transport and thermal conduction losses to its surroundings. Used in a pump-probe experiment, this new approach has enabled the first single-state measurement of electrical conductivity of gold at energy densities of 2.8×10^5 to 2.2×10^7 J/kg. At the same time, the study reveals a quasi-steady-state behavior in the electrical conductivity of the sample following laser excitation. This hints at the existence of a metastable liquid phase over picosecond time scales. The study also shows the onset of disassembly of the heated sample, indicative of a liquid-plasma transition.

In this Letter, we present a study of the temporal behavior of the optical properties of gold under ultrafast laser excitation. This is used to assess nonequilibrium melting and liquid-plasma transitions over a wide range of excitation energy densities. The study employs a variety of pump-probe diagnostics including reflectivity, transmissivity, and phase shift to provide measurements with different sensitivity to density gradient and hydrodynamic expansion. Our results confirm the quasistability of the liquid phase that follows nonthermal melting. They also identify the liquid-plasma transition together with a measurement of the energy density threshold for the transition. In the experiment, 25–30 nm thick freestanding gold foils are heated with 150 fs full width at half maximum (FWHM), 400 nm laser pulses at normal incidence. Spatial resolution of the diagnostics is 5 μm. The excitation energy density is determined from the measured reflectivity and transmissivity of the pump laser. To examine the optical properties of the heated sample, six different diagnostics are used. Two of these provide measurements of reflectivity and transmissivity of an *S*-polarized, 150 fs FWHM, 800 nm laser probe incident at 45° to the normal of the foil target [9]. For a more sensitive diagnostic of density gradient and hydrodynamic expansion, the polarization of the probe is rotated by 90°. The reflectivity and transmissivity of the *P*-polarized probe are governed by not only the dielectric function of the heated foil but also resonant absorption at critical density [10]. To provide a more direct interrogation of hydrodynamic expansion, frequency domain interfer-

ometry (FDI) [11] is used with the *S*- or *P*-polarized probe. This measures the change in phase shift, $\Delta\Phi$, of the specularly reflected light. The value of $\Delta\Phi$ is determined by both dielectric function of the sample and motion of the critical density layer when hydrodynamic expansion occurs.

Figure 1 shows the temporal evolution in the optical properties of the femtosecond laser heated gold foil. For all diagnostics, time zero is defined by the onset of detectable changes in the *P*-polarized probe reflectivity because it shows the highest percentage change to laser heating. It is remarkable that they all exhibit the same three stages of temporal evolution. The response of the foil to laser excitation begins with a transient that extends to $t \sim 1.5$ ps. This is followed by a quasisteady state that lasts approximately 3.5 ps before the onset of another rapid change. These results clearly confirm the quasisteady state behavior and its interpretation as the absence of significant hydrodynamic expansion. Otherwise, it would require the spatially varying dielectric property of an expanding foil to evolve in such a manner to mitigate precisely effects due to density gradient or hydrodynamic flow for the entire duration of the quasisteady state. This is highly improbable. The FDI measurement is particularly noteworthy. It provides direct evidence of hydrodynamic expansion subsequent to the quasisteady state. Furthermore, its sensitivity to expansion renders it the best monitor of the quasisteady state behavior. This is illustrated in Fig. 2, which examines the phase shift data in the vicinity of the quasisteady state.

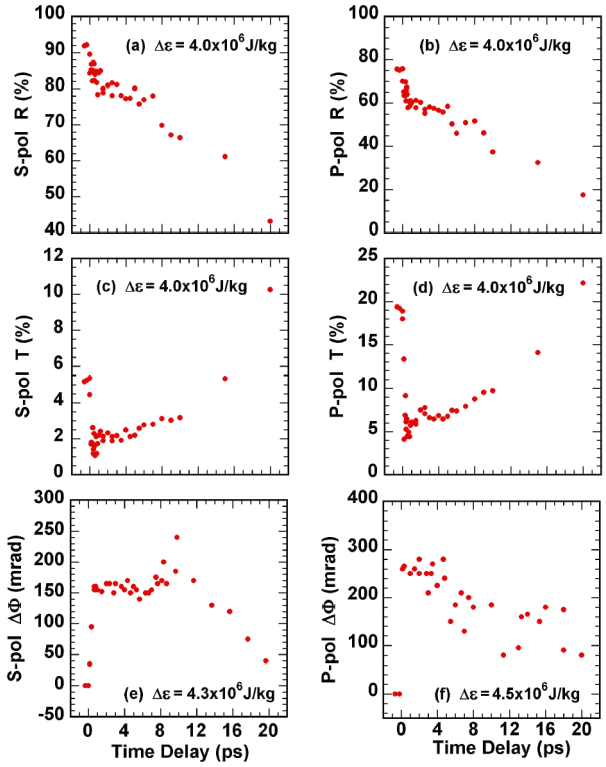

FIG. 1 (color online). Temporal evolution of optical properties for $\Delta\varepsilon$ of (4.0–4.5) $\times$ 10^6 J/kg.

To understand the behavior of the optical properties of gold under ultrafast laser excitation, we examine first its dielectric function. Figure 3 shows an example for an excitation energy density of 4.0×10^6 J/kg. The results are derived from *S*-polarized reflectivity and transmissivity measurements for uniform, isochoric heating conditions as described before [9]. Time zero is again defined by the onset of detectable changes in the *P*-polarized reflectivity. The dielectric function displays the same characteristic signature of a transient response that lasts for ~1.5 ps, followed by a quasisteady state to $t \sim 5$ ps. Beyond that time, disassembly of the foil gives rise to gradients that render it invalid to derive dielectric function from reflectivity and transmissivity data through solutions to the Helmholtz equations [9]. During the transient, the dielectric function reaches the equilibrium liquid value within the first 200 fs. This is much faster than the ~500 fs observed in aluminum heated at a much lower laser fluence [5]. Such a behavior has been attributed to nonthermal melting where electronic excitation causes weakening of bonds. Our data would suggest that, in the high excitation energy density or strongly overdriven regime, nonthermal melting takes place in a much faster time scale. On the other hand, the ~600 fs needed to reach the local minimum or maximum in ϵ_r or ϵ_i is dictated by the laser heating process since 95% of the pulse energy is contained within that duration. Then, it takes a further ~900 fs for the dielectric function to relax to a quasisteady state value. Like conductivity, dielectric function is governed by both the electron-ion scattering cross section and the ion structure factor [12]. In the regime of interest here, the scattering cross section is dictated by the electron Fermi speed, which is a function of electron density only. Thus, the relaxation of the dielectric function is a manifestation of changes in

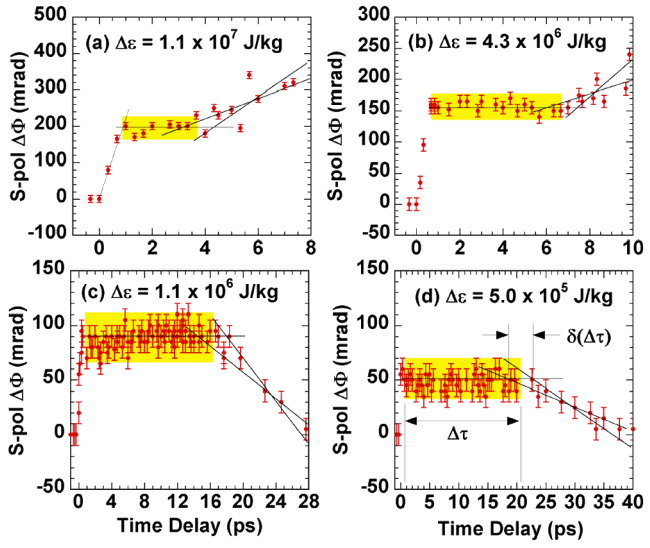

FIG. 2 (color online). FDI data showing the duration of the quasisteady state (shaded area). The error bars are uncertainties due to the noise level of the measurement. The solid lines are for guidance and illustrate the time-value extraction for Fig. 4(a).

the ion structure factor as the lattice relaxes into a liquid structure. The time scale of relaxation is slightly faster than the 3.5 ps found in ultrafast electron diffraction measurements on femtosecond laser heated aluminum at a lower laser fluence [7]. The electron diffraction study also shows that the structure factor of the nonequilibrium liquid remains unchanged for tens of picoseconds. This can readily explain our observation of quasisteady state behavior of the dielectric function for several picoseconds. From Fig. 3 it is evident that the quasisteady state dielectric function is significantly different from that of an equilibrium gold liquid. This is due to the substantial excited electron population that exists in the nonequilibrium liquid at high excitation energy densities.

Turning to the hydrodynamic disassembly of the heated foil, we study the dependence of the onset of hydrodynamic expansion on excitation energy density. We define the time scale for disassembly, $\Delta\tau$, as the period between the end of laser heating that is signaled by the local minimum or maximum of the transient optical property and the onset of expansion that is signaled by the subsequent rapid change in optical property. For this analysis we use S-polarized FDI data that offer the clearest temporal signature as discussed above and illustrated by Fig. 2 which also shows the observed quasisteady state durations. The results are presented in Fig. 4(a). Interestingly, the observed functional dependence can be explained quite well with the widely used two-temperature model [13]. This model treats electrons and lattice as two subsystems, each characterized by a temperature. Thermal equilibration between them is governed by a coupling constant g. In their original form, the model equations are

$$C_e \frac{dT_e}{dt} = -g[T_e - T_l] + S_L(t), \tag{1}$$

$$C_l \frac{dT_l}{dt} = g[T_e - T_l], \tag{2}$$

where $S_L(t) = \Delta\varepsilon\rho_{\mathrm{Au}}/(t_w\sqrt{\pi})\exp[-(t-t_0)^2/t_w^2]$ describes the deposition of the femtosecond laser pulse, $t_0 = 300$ fs is the time for peak laser intensity, $t_w = 150$ fs is FWHM, g is the electron-phonon coupling constant, C_e is the electron heat capacity calculated from the temperature dependent chemical potential [14], and $C_l = 2.5 \times 10^6\ \mathrm{J\,m^{-3}\,K^{-1}}$ is the lattice heat capacity [15]. To allow for solid-liquid and liquid-vapor transitions, we have replaced the lattice temperature equation with that for lattice energy density ε_l to take into account implicitly the unknown latent heat of fusion and vaporization,

$$C_e \frac{dT_e}{dt} = -g\left[T_e - \varepsilon_l \frac{\rho_{\mathrm{Au}}}{C_l}\right] + S_L(t), \tag{3}$$

$$C_l \frac{dT_l}{dt} = g\left[T_e - \varepsilon_l \frac{\rho_{\mathrm{Au}}}{C_l}\right]. \tag{4}$$

The density of gold ρ_{Au} is 19.3 $\mathrm{g/cm^3}$. In our calculation, the lattice specific heat is assumed to remain unchanged for the liquid phase. Figure 4(b) shows results of our calculation for an excitation energy density of 4.0×10^6 J/kg. A value of $g = 2.2 \times 10^{16}\ \mathrm{W\,m^{-3}\,K^{-1}}$ is used based on results of extensive measurements for fluences up to 130 $\mathrm{mJ/cm^2}$ [16]. Peak electron temperature appears at time τ_H to correspond to the end of laser heating. The onset of hydrodynamic disassembly is marked by τ_D in the figure. Accordingly, $\Delta\tau = (\tau_D - \tau_H)$. During the quasisteady state period, the lattice energy density increases substantially with only a minor decrease in electron temperature. This is due to the assumed linear dependence of electron specific heat on temperature in the model. Using Fig. 4(b), $\Delta\tau$ can be correlated with a critical lattice energy density ε_D. If the disassembly of the nonequilibrium liquid is independent of the rate of energy transfer to the lattice,

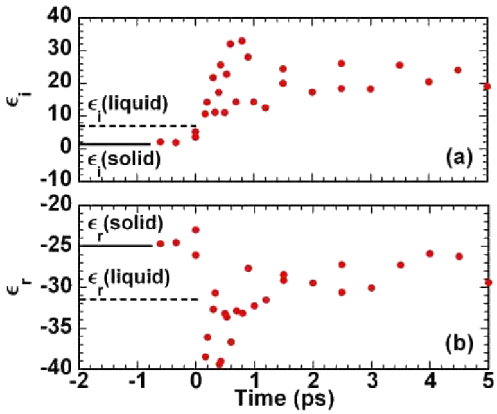

FIG. 3 (color online). Temporal evolution of dielectric function for $\Delta\varepsilon = 4.0 \times 10^6$ J/kg.

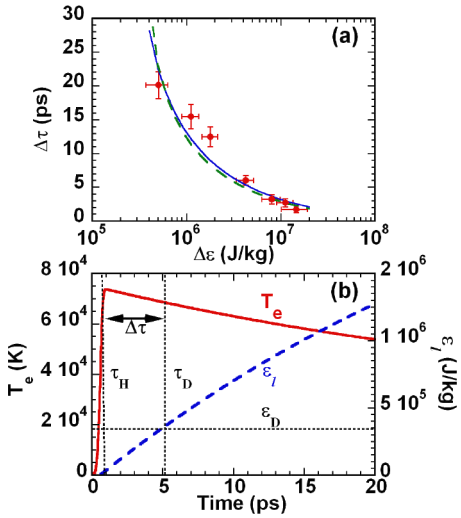

FIG. 4 (color online). (a) Duration of quasisteady state phase as a function of excitation energy density for g of $1.9 \times 10^{16}\ \mathrm{W\,m^{-3}\,K^{-1}}$ (solid line) and $2.5 \times 10^{16}\ \mathrm{W\,m^{-3}\,K^{-1}}$ (dashed line). (b) Calculated temporal evolution of electron temperature and lattice energy density for $\Delta\varepsilon = 4.0 \times 10^6$ J/kg and $g = 2.2 \times 10^{16}\ \mathrm{W\,m^{-3}\,K^{-1}}$.

the same ε_D should apply to observations made at all excitation energy densities. With this hypothesis, we find values of ε_D to yield the best fit curves for the data in Fig. 4(a). It is evident that there is reasonable agreement between the simple model and experiment. For the reported value of $g = (2.2 \pm 0.3) \times 10^{16}$ W m^{-3} K^{-1} our result yields $\varepsilon_D = (3.3 \pm 0.3) \times 10^5$ J/kg.

To understand the process responsible for disassembly of the nonequilibrium liquid, we examine first the temporal behavior in phase shift $\Delta\Phi$ determined from *S*-polarized FDI measurements. As illustrated in Fig. 1(e), the increase in $\Delta\Phi$ at the onset of disassembly is indicative of an expanding plasma in which the critical density layer moves towards the probe source. This is followed by a decrease in $\Delta\Phi$ when density reduction in the expanding region dominates. Such two processes become much less distinguishable at lower excitation energy densities as evident in Figs. 2(c) and 2(d), depending on the interplay between them.

In addition, we measure the time scale for disassembly, $\Delta\tau$ as a function of background pressure from 3×10^{-5} Torr (vacuum) to 100 Torr (helium). The onset of target disassembly is found to be independent of the surrounding pressure. This means that the critical energy density ε_D for disassembly is also independent of background pressure. This is different from the process of vaporization of a neutral liquid under equilibrium conditions where the phase boundary is dictated by vapor pressure. For gold under ultrafast laser excitation, the nonthermally melted liquid is metallic with a significant population of excited electrons. When it vaporizes, the gas phase is thus a plasma. The dynamics of disassembly is dictated by the plasma electron pressure that can readily exceed several hundred kbar [17]. These observations therefore suggest that the disassembly of the nonequilibrium liquid is the result of a liquid-plasma transition.

While first-principle calculations of phase transitions and dynamical changes in optical properties of gold under ultrafast laser excitation are not available, it is instructive to present a qualitative discussion of the processes involved. Laser absorption creates initially a highly nonequilibrium density of state for the electrons as they are excited by the 3 eV photons from either the s/p or the d band to levels above the Fermi surface. Deexcitation via electron-hole recombination and thermalization via electron-electron scattering lead to a Fermi-Dirac distribution. This is expected to occur in subpicosecond time scales [18]. At the same time the high degree of electronic excitation can cause weakening of bonds, thus reducing the stability of the lattice and giving rise to nonthermal melting [19]. Another coexisting but minor process is the excursion of the excited electrons into the surrounding vacuum because of electron pressure. This is, however, limited by space charge effect that allows only an electron plasma sheath to be formed on the surface of the foil. The thickness of such a sheath would be less than 1 nm for electron energy pertinent to this study. Amid all these processes, electron-phonon coupling begins to heat the lattice. The material will remain as a nonequilibrium liquid until sufficient energy is transferred to the lattice to effect vaporization. Since the nonthermally melted gold is a charged liquid, its vaporization leads to the formation of a gaseous plasma that can expand freely subject to ambipolar diffusion [20] of the electrons and ions.

In conclusion, we have used the temporal behavior of the optical properties of gold to examine nonequilibrium phase transitions induced by ultrafast laser excitation at energy densities up to 2×10^7 J/kg. The initial transient response in the dielectric function is consistent with nonthermal melting followed by the relaxation of the lattice to a liquid structure. The subsequent quasisteady state phase is attributed to a nonequilibrium liquid dominated by an excited electron distribution. Disassembly of the liquid into a plasma phase is found to occur at a lattice energy density of $(3.3 \pm 0.3) \times 10^5$ J/kg independent of the laser excitation energy density and background pressure. This provides the first observation of nonequilibrium liquid-plasma transition in a strongly overdriven regime.

This work was performed under the auspices of the U.S. Department of Energy by University of California Lawrence Livermore National Laboratory under Contract No. W-7405-ENG-48 and was supported by the Natural Sciences & Engineering Research Council of Canada.

[1] C. V. Shank *et al.*, Phys. Rev. Lett. **51**, 900 (1983).
[2] H. W. K. Tom *et al.*, Phys. Rev. Lett. **60**, 1438 (1988).
[3] P. Saeta *et al.*, Phys. Rev. Lett. **67**, 1023 (1991).
[4] C. W. Siders *et al.*, Science **286**, 1340 (1999).
[5] C. Guo *et al.*, Phys. Rev. Lett. **84**, 4493 (2000).
[6] A. Rousse *et al.*, Nature (London) **410**, 65 (2001).
[7] B. J. Siwick *et al.*, Science **302**, 1382 (2003).
[8] V. Schmidt *et al.*, Phys. Rev. Lett. **85**, 3516 (2000).
[9] K. Widmann *et al.*, Phys. Rev. Lett. **92**, 125002 (2004).
[10] V. L. Ginzburg, *Propagation of Electromagnetic Waves in Plasmas* (Gordon and Breach, New York, 1961).
[11] J. P. Geindre *et al.*, Opt. Lett. **19**, 1997 (1994).
[12] J. M. Ziman, Philos. Mag. **6**, 1013 (1961).
[13] S. I. Anisimov *et al.*, Sov. Phys. JETP **39**, 375 (1974).
[14] T. C. Dorlas, *Statistical Mechanics: Fundamentals and Model Solutions* (IoP Publishing, Bristol, 1999), p. 187.
[15] A. M. James and M. P. Lord, *Maxmillian's Chemical and Physical Data* (Maxmillian Press, London, 1972).
[16] J. Hohlfeld *et al.*, Chem. Phys. **251**, 237 (2000).
[17] Sesame tabular equation of state, Los Alamos National Laboratory, Material No. 2700 (unpublished).
[18] E. J. Yoffa, Phys. Rev. B **21**, 2415 (1980).
[19] J. V. Van Vechten, Phys. Lett. **74A**, 422 (1979).
[20] F. F. Chen, *Introduction to Plasma Physics and Controlled Fusion* (Plenum Press, New York, 1984), 2nd ed., Vol. 1, p. 159.